

BEE 453: COMPUTER AIDED ENGINEERING

Professor Ashim K. Datta

May 7, 2004

Heat Transfer in Laser Tumor Excision



Submitted by

Alan Chen, Edwin Cheung, Steven Lee, John Picuri, Tsung Li Shih

Contents

Executive Summary.....	3
Realistic Constraints.....	3
Introduction.....	4
Design objectives.....	4
Schematic.....	4
Results and Discussion.....	5
Sensitivity Analysis.....	9
Conductivity.....	11
Convection.....	12
Specific Heat.....	13
Laser Power.....	15
Conclusions.....	16
Appendix A.....	16
Geometry.....	16
Governing Equation.....	16
Initial and boundary conditions.....	17
Constant Tissue Properties.....	17
Appendix B.....	18
PROBLEM Statement keywords.....	18
SOLUTION Statement.....	18
TIMEINTEGRATION statement.....	18
Convergence analysis.....	18
Appendix D.....	19

Executive Summary

Cancer is an ongoing disease that is present in a majority of the population. Laser surgery provides minimally invasive techniques to excise tumors in humans. This method allows quicker recoveries and fewer complications. This study analyzes the effectiveness of excision of tumor tissue using a CO₂ laser. By using computer aided design and finite element analysis, we model a cylindrical tumor tissue with 0.3cm in diameter and height. A flux of $82 \frac{W}{mm^2}$ from the laser and a convection coefficient of $5 \times 10^{-6} \frac{W}{mm^2 \cdot K}$ were applied when designing this model. Our results produced temperature contour plots at several time intervals, all showing precise laser excision with minimal inadvertent tissue damage (less than 0.006 mm in depth after excising approximately 0.15 mm of tissue in depth). Sensitivity analysis indicate that changes in material properties such as conductivity, convection, specific heat, density, and laser power have minimal affects on the temperature profile.

Realistic Constraints

When dealing with technological advances in society, we must address that fact the existence of constraints limiting the success of that technology. The laser discussed in our study has two main constrains: health and safety constrains and social constraints.

As with all medical surgical tools, there is always the risk of complications due to technical malfunction or human error. The constraints for laser surgery dealing with complication are hemorrhaging, infection, perforation, destruction of healthy tissue, scarring, change in skin pigmentation, etc. With exception to the last health constraint, all the others relate to problems existing in even conventional surgical procedures involving scalpels and scissors.

Social constrains also exist in the sense that complication in surgery may cause disfiguration or pain. When treating tumors, scarring or changes in skin pigmentation may disrupt a patient emotionally. Complications causing pain or permanent injuries may prevent a person going to work or enjoying social occasions. However, when surgeries proceed normally, patients benefit from shorter recover times, allowing them to return to their lives quicker and more comfortably.

Other constraints in laser surgery are the lack of physicians trained to perform laser surgery. In-office surgical procedures give rise to the complication of distant emergency facilities in the case of complications. Other constraints include necessary eyewear precautions and expensive, bulky laser equipment.

Introduction

Cancer is an ongoing disease that is present in a majority of the population. In fact, it is the second leading cause of death in the United States. When body cells begin to grow out of control, cancer develops in the body. These cancer cells outlive normal cells and continue to form new abnormal cells usually resulting in a tumor. There are four major types of cancer treatment. They are surgery, radiation, chemotherapy and biologic therapies[1]. For tumors present topically, laser surgery is a moderately simple yet effective method to remove the cancerous tissue. It uses high-intensity light to excise the tissue surrounding the tumor allowing physical removal of the cancerous tissue. Even though there are several different kinds of lasers, CO₂ laser, Nd:YAG laser and Argon laser are the ones that are widely used in medicine[2].

Of the many types of tumors, head and neck cancers are the ones most treated using laser surgery. These types of cancers make up 5% of the total cancer cases in the United States and previously could only be treated using laser surgery when in the localized (Stage I) phase. Advancements, however, have allowed treatment of deeper tumors which allows the several advantages laser therapy (such as high precision[3], pain reduction, swelling reduction, control of infection and minimal surgical bleeding[4]) to be used on a wider range of ailments.

In laser therapy, laser is used as an excision tool, cutting out portions of cancerous tissue. It transfers large amount of heat to the target area causing vaporization of the tissue surrounding the tumor. During the heating process, however, other surrounding healthy tissues might also be affected. Because of this, it would be advantageous to model the heat transfer process during laser surgery. This will allow us to determine the optimal laser power and the extent of tissue damage.

Design objectives

The main objective of laser excision is to excise the tumor with minimally invasive procedures. In our project, we are modeling the heat transfer from the laser to the surrounding healthy tissue. With the model, we can determine the extent of tissue damage during tumor removal. GAMBIT was used to create a mesh modeling the tissue to be excised and surrounding tissue. FIDAP was then used to model the thermal characteristics surrounding the laser excision in order to determine the amount of damage done to the surrounding tissue during the excision. We will also perform sensitivity analysis on the tissue conductivity, tissue specific heat, convection of tissue surface, tissue density, and laser power.

Schematic

The tissue will be modeled as a cylinder of uniform density and conductivity. The region of concern is the cylindrical volume near the laser targeted area. The cylinder is 0.3mm in radius and 0.3mm in height. The schematic of the model can be found at Appendix A.

Results and Discussion

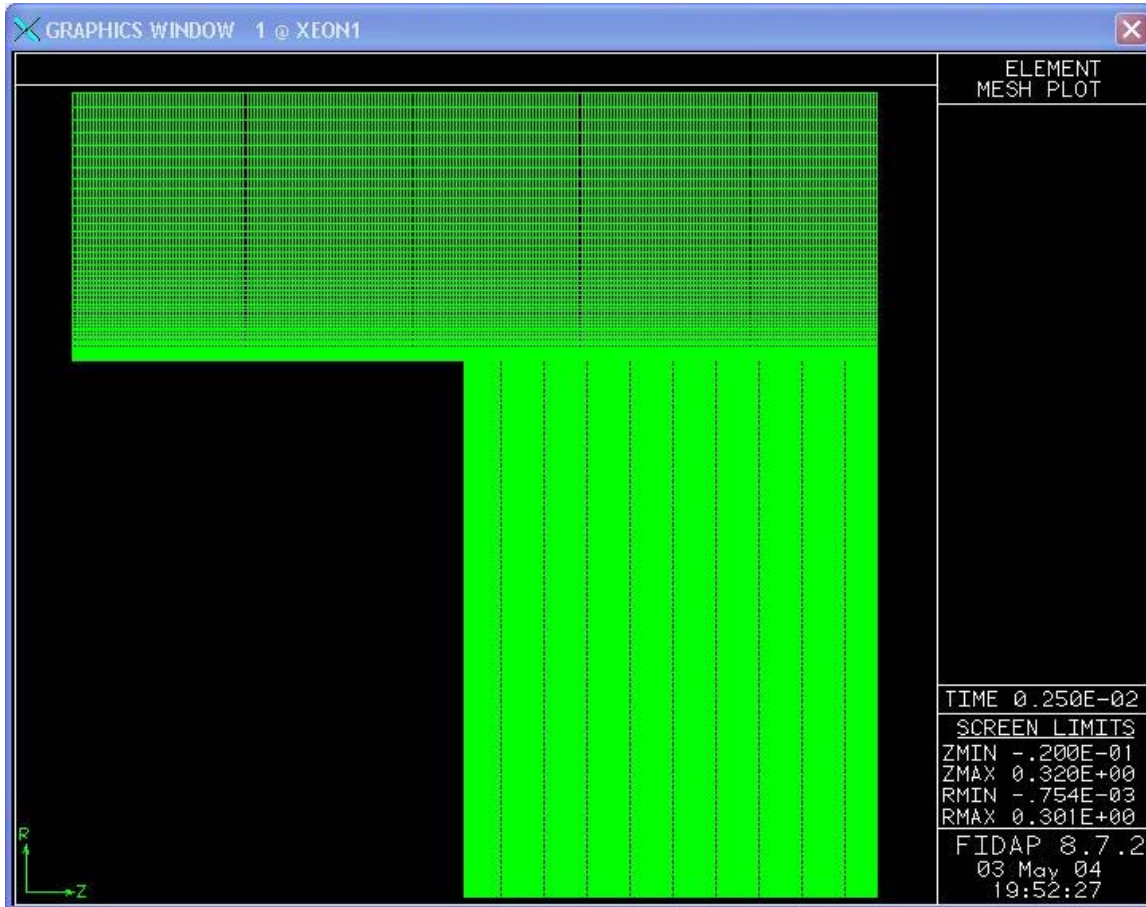


Figure 1: Mesh at 2.5 milliseconds. Note that the region of “burn” is compressed and contains a greater density of nodes. The model of the simulation does not actually remove any nodes during “excision” and instead compresses the nodes.

In order to model the excision of tissue, a moving boundary layer was implemented. The 0.2 mm mesh area below the laser was compressed to represent the removal of tissue. It is important to recognize that no actual elements of the mesh are being removed, the elements are only being compressed.

A physical approximation error is introduced in this model because nodes initially adjacent remain adjacent throughout the test. Therefore on the boundary of the excision, the surface of the undamaged tissue side as well as the surface of the excision side is considered adjacent. The finite element analysis will cause these two nodes to interact with each other as if they were still physically linked. This created some anomalies at the border of the excision.

The speed of the moving boundary was determined by first using a fixed boundary shown below in Figure 2. The depth of tissue damage (based on the 150°C threshold) over the time set the rate of damage propagation and determined the moving boundary rate in our subsequent trials.

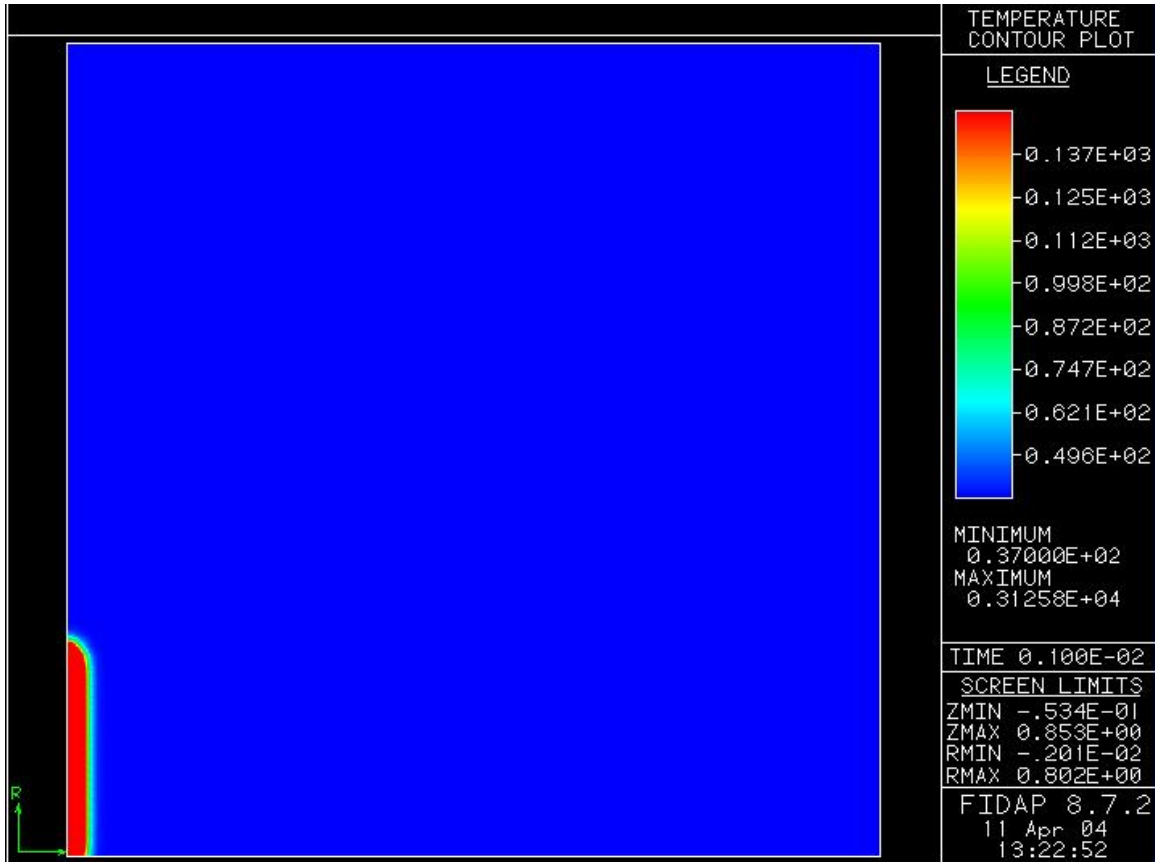


Figure 2: Fixed boundary test.

The computer generated scenario was simulated with a laser flux of $82 \frac{W}{mm^2}$. The model took into account for the heat convection of $5 \times 10^{-6} \frac{W}{mm^2 \cdot K}$. The red contour in Figure 3 shows the surrounding tissue where the temperature of the tissue exceeded $50^\circ C$. While $50^\circ C$ is a somewhat arbitrary temperature designation (especially considering it would take a significant period of time to develop burn damage at this temperature) we believed that any tissue under this temperature would definitely not be damaged which allows some qualitative determination of tissue damage. While the tissue at $50^\circ C$ will be damaged slightly, all of the tissue with temperature above $50^\circ C$, which is most of tissue between the $50^\circ C$ boundary and the excision edge, will be damaged quite excessively. The red zone above $50^\circ C$ is noticeably thin, which indicates that tissue excision is controlled and little surrounding tissue is destroyed during the process. Tissue outside this red zone region remains close to the initial conditions $37^\circ C$ and is not likely to be harmed by the laser excision process.

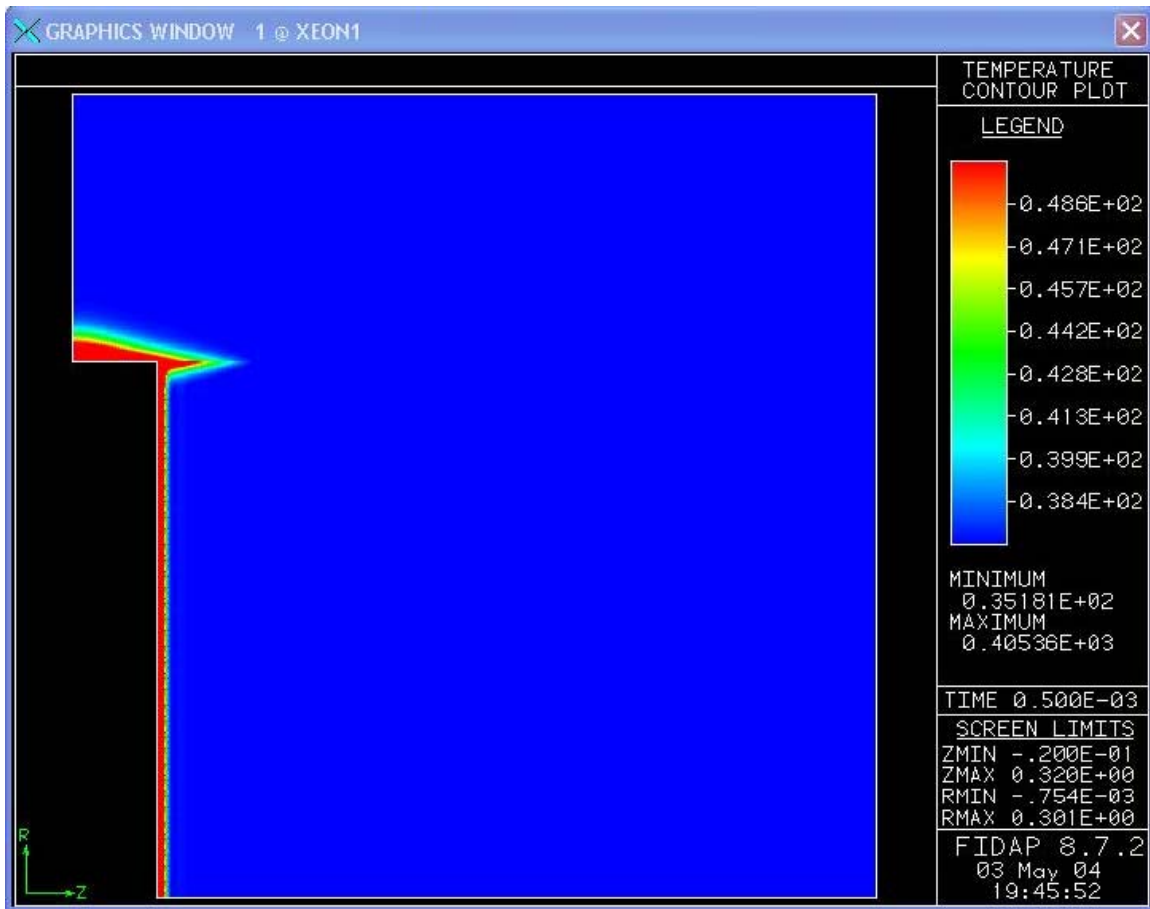


Figure 3: Temperature contour plot of tumor after 0.5 milliseconds.

Figure 4 below displays the temperature contour plot of the tissue after 2.5 milliseconds. We can see that the laser burned tissue deeper, proceeding in the z direction. Again the red region where tissue is destroyed is thin, showing that the burning of surrounding tissue is minimized.

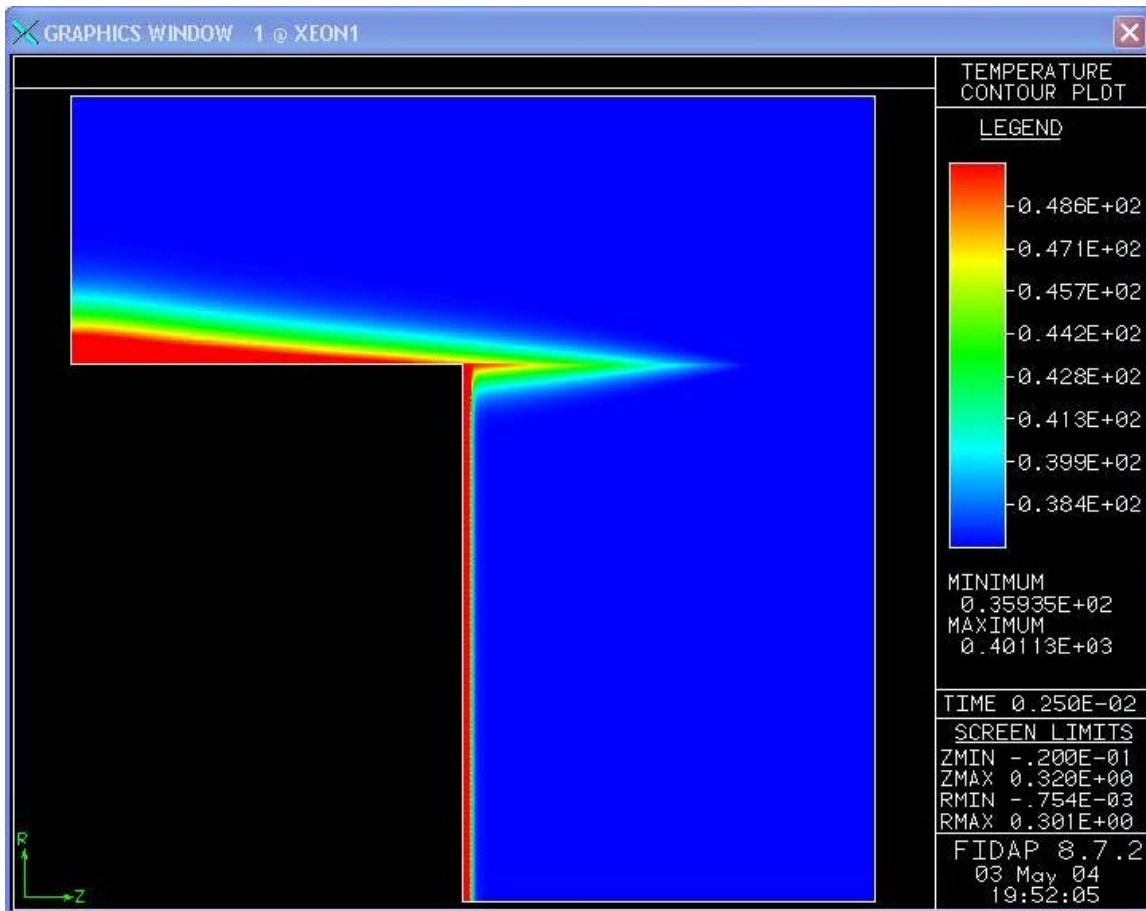


Figure 4: *Temperature contour plot of tumor after 2.5 milliseconds.*

Sensitivity Analysis

In order to determine the effect of the various properties on the solution, the values of conductivity, convection, specific heat, density, and laser power were varied from the accepted value and temperature contour plots were compared for the tissue.

One of the major assumptions of our model was constant tissue properties. However in actuality, the density and conductivity would be a function of temperature.

The conductivity sensitivity analysis showed very little variation. The 10% increase (Figure 5) shows a small green contour line that is not present in the other two lower conductivity plots. This temperature still reflects a value below the damage threshold and will therefore have minimal results on data interpretation. Convection, specific heat and density all showed similar results with little sensitivity. Therefore errors in our initial assumptions will have little impact on our results.

Intuitively, the laser power should have an impact on the tissue destruction and temperature profile. Figures 17-19 demonstrate different energy fluxes at different times (normalized by changing the speed of the moving boundary). The similarity in the temperature profiles demonstrate that the laser power will not change the extent of tissue damage, only the speed at which it occurs. This has implications in both giving validity to our assumed laser power and in laser excision techniques.

Conductivity

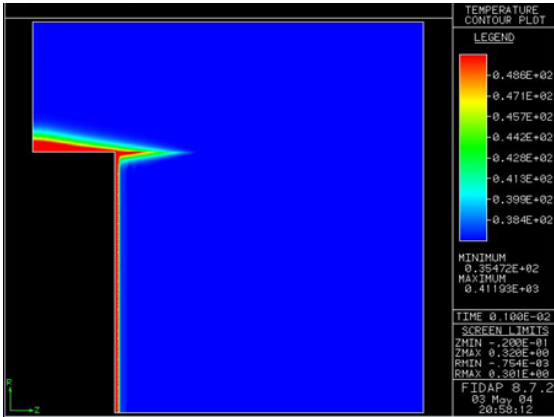


Figure 5: Temperature contour plot with conductivity value of $0.1881 \times 10^{-3} \frac{W}{m \cdot K}$.

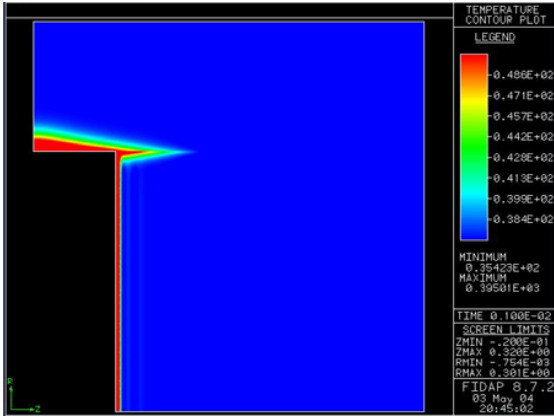


Figure 6: Temperature contour plot with conductivity value of $0.2209 \times 10^{-6} \frac{W}{m \cdot K}$.

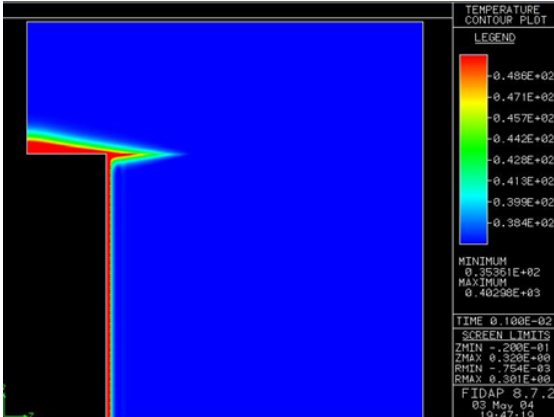


Figure 7: Temperature contour plot with conductivity value of $0.2299 \times 10^{-6} \frac{W}{m \cdot K}$.

Convection

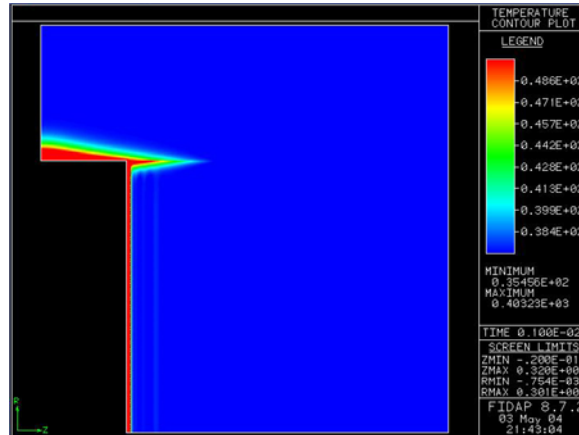


Figure 8: Temperature contour plot with convection value of $25 \times 10^{-6} \frac{W}{mm^2k}$.

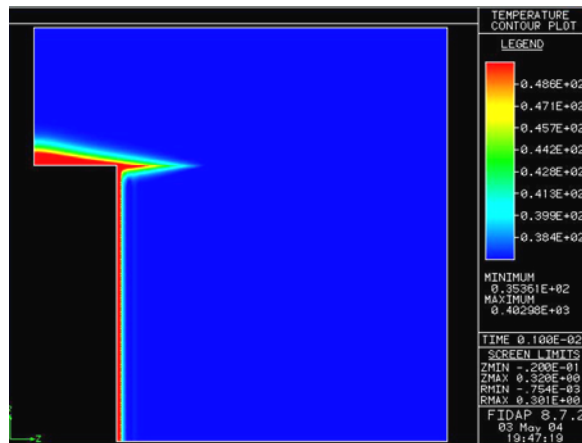


Figure 9: Temperature contour plot with convection value of $5 \times 10^{-6} \frac{W}{mm^2k}$.

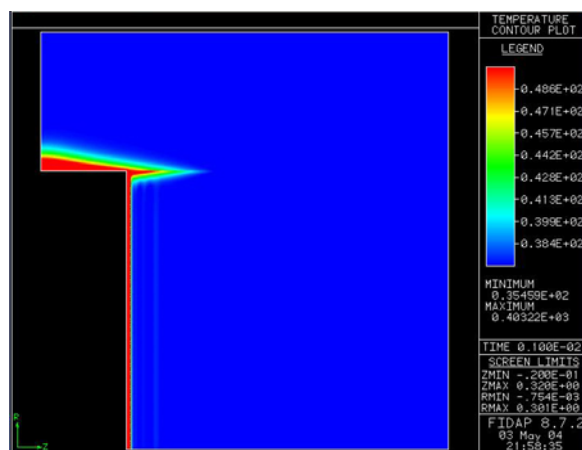


Figure 10: Temperature contour plot with convection value of $50 \times 10^{-6} \frac{W}{mm^2k}$.

Specific Heat

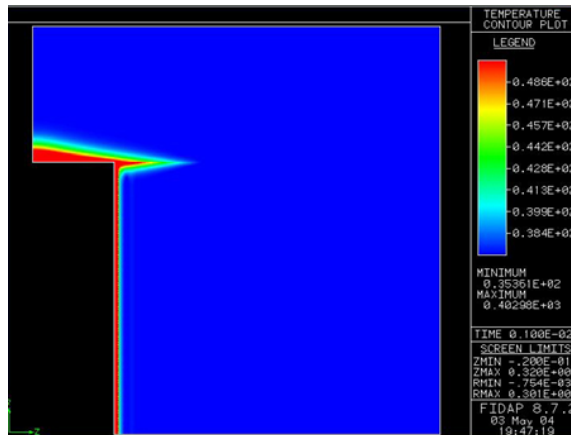


Figure 11: Temperature contour plot with specific heat value of $3768.3 \frac{J}{g \cdot ^\circ C}$.

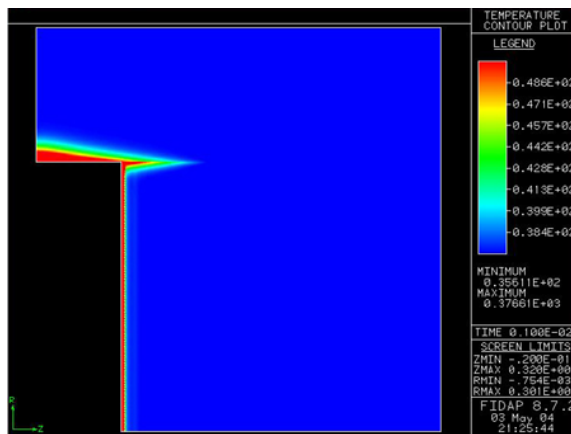


Figure 12: Temperature contour plot with specific heat value of $4178.0 \frac{J}{g \cdot ^\circ C}$.

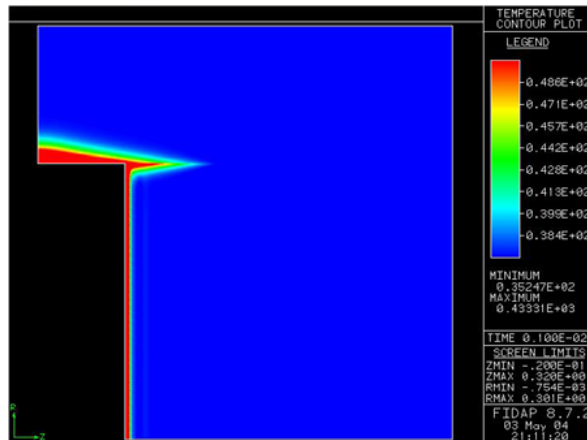


Figure 13: Temperature contour plot with specific heat value of $4605.7 \frac{J}{g \cdot ^\circ C}$.

Density

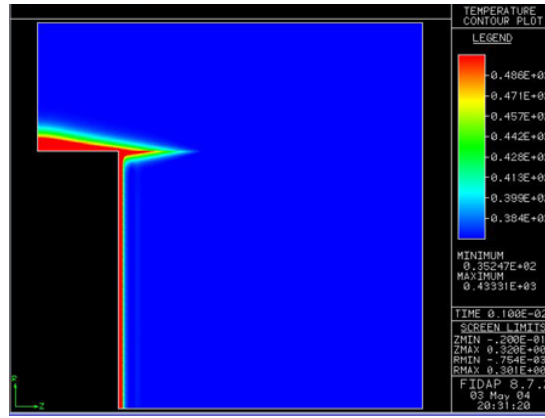


Figure 14: Temperature contour plot with density value of $0.9 \times 10^{-6} \frac{kg}{cm^3}$.

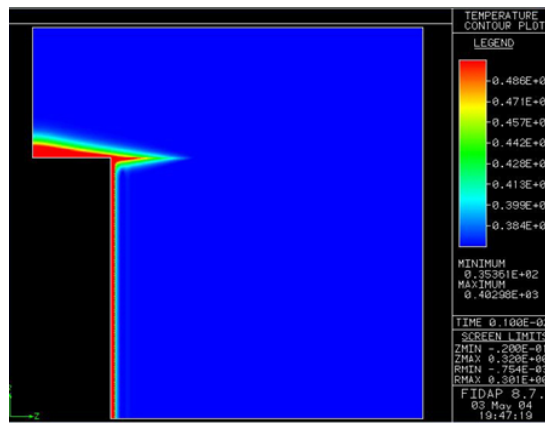


Figure 15: Temperature contour plot with density value of $1.0 \times 10^{-6} \frac{kg}{cm^3}$.

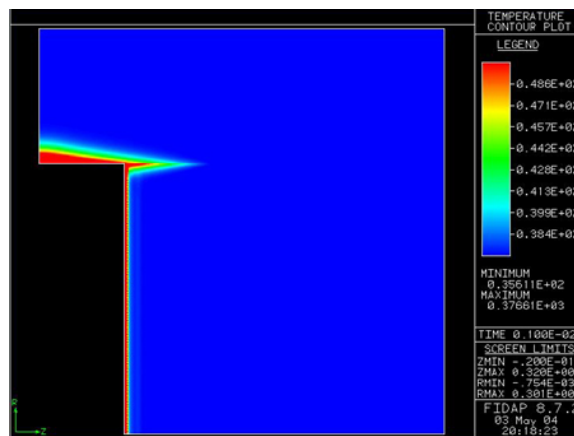


Figure 16: Temperature contour plot with density value of $1.1 \times 10^{-6} \frac{kg}{cm^3}$.

Laser Power

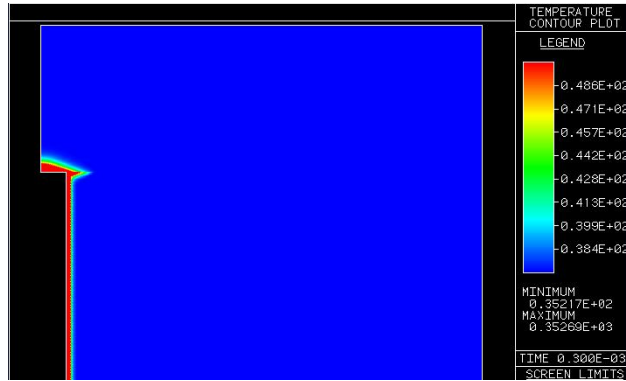


Figure 17: Temperature contour plot with laser power value of 9W.



Figure 18: Temperature contour plot with laser power value of 12W.



Figure 19: Temperature contour plot with laser power value of 15W.

Conclusions

The relatively small degree of incidental tissue damage or destruction demonstrates that laser excision is a highly precise process. The sensitivity analysis of tissue conduction, convection, specific heat, density, and laser power validates our assumptions and properties. The results from the sensitivity analysis also show that laser power has very little effect on the temperature profile once the speed of excision is accounted for.

Appendix A

Geometry

The site of laser excision is modeled as a cylinder of homogenous tissue with both a radius and height of 0.3mm. Due to the large energy flux over a short time period, it was reasoned that significant heating would not occur in regions outside of the model.

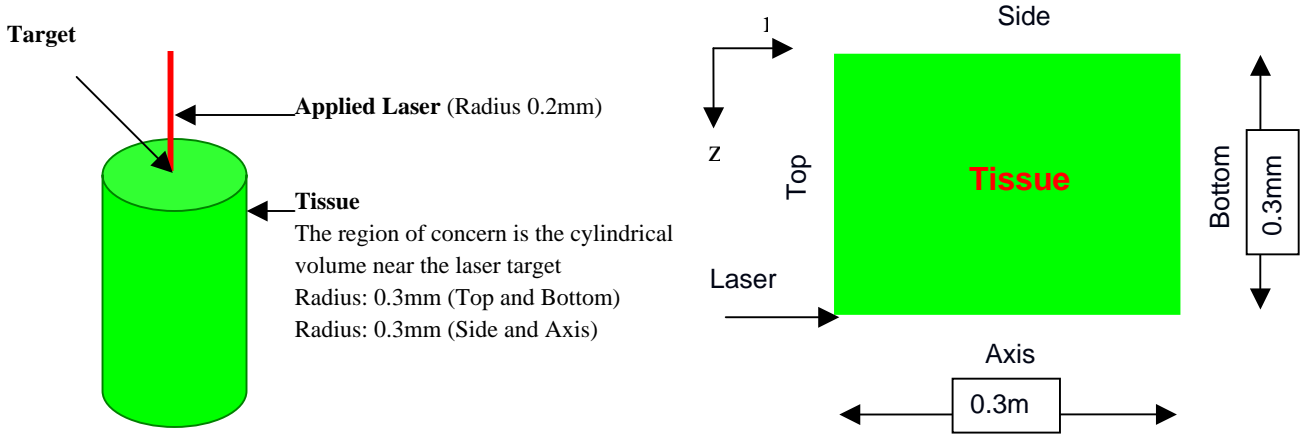


Figure 20: Schematic of the geometry.

An axis symmetrical model was used with the center of the tissue as the axis. Heat transfer in this model only occurs in the r and z directions.

Governing Equation

In modeling energy transfer in cylindrical coordinates, the governing equation is:

$$\rho C_p \left(\frac{\delta T}{\delta t} + v_r \frac{\delta T}{\delta r} + \frac{v_\theta}{r} \frac{\delta T}{\delta \theta} + v_z \frac{\delta T}{\delta z} \right) = k \left[\frac{1}{r} \frac{\delta}{\delta r} \left(r \frac{\delta T}{\delta r} \right) + \frac{1}{r^2} \frac{\delta^2 T}{\delta \theta^2} + \frac{\delta^2 T}{\delta z^2} \right] + Q$$

Since there are no variations in temperature in the θ direction and there is no internal flow, the equation reduces to:

$$\rho C_p \frac{\delta T}{\delta t} = k \left[\frac{1}{r} \frac{\delta}{\delta r} \left(r \frac{\delta T}{\delta r} \right) + \frac{\delta^2 T}{\delta z^2} \right]$$

Initial and boundary conditions

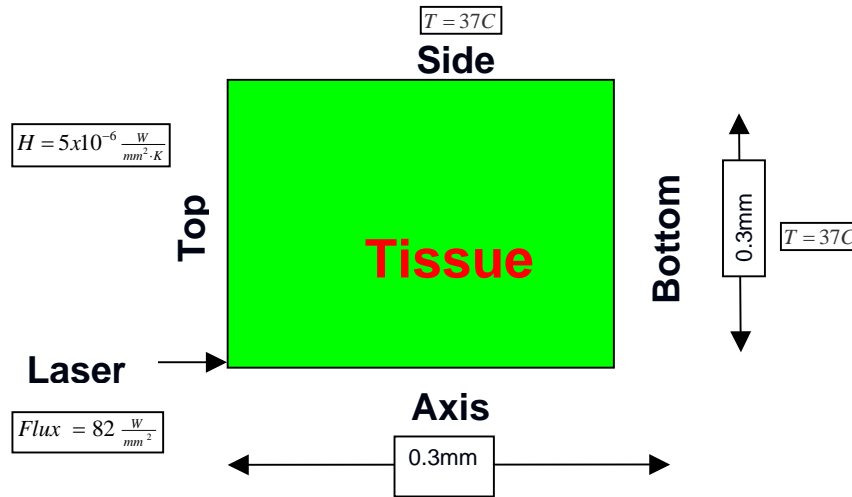


Figure 21: Schematic of the geometry with initial condition.

The sides and bottom of the tissue were assumed to be thoroughly buffered by the adjacent tissue outside of the geometry and therefore kept at the constant temperature of $37^\circ C$. The laser has a constant energy flux of $82 \frac{W}{mm^2}$. The top surface is affected by convective transfer with $H = 5 \times 10^{-6} \frac{W}{mm^2}$.

Constant Tissue Properties

- Conductivity: $2.09 \times 10^{-3} \frac{W}{mm \cdot K}$
- Density: $1 \times 10^{-5} \frac{kg}{mm^3}$
- Specific Heat: $4,187 \frac{J}{kg \cdot K}$

Appendix B

PROBLEM Statement keywords

Geometry type	Axi-symmetric	The tumor model is symmetric across the axis, so only one calculation is needed to interpret the result.
Flow regime	Incompressible	Not important because there is no flow in our model.
Simulation type	Transient	The result depends on time.
Flow type	Laminar	Not important because there is no flow in our model.
Convective term	Linear	Not important because there is no flow in our model.
Fluid type	Newtonian	Not important because there is no flow in our model.
Momentum equation	Momentum	In real life, we do not need to use momentum equation. However, we need to use momentum equation in our model because of the moving boundary.
Temperature dependence	Energy	The energy term accounts for the thermal conduction.
Surface type	Free	Due to our moving boundary.
Structural solver	None	There is no structural solver.
Elasticity remeshing	No remeshing	There is no remeshing.
Number of phases	Single phase	There is only matter of a single phase.
Species dependence	Species = 0	Including burnt tissue cause problems in the model so we did not include this in this reports conclusions

SOLUTION Statement

Solution method	QuasiNewton = 10	This setting solves the problem with a maximum of 10 iterations for any one time step.
Relaxation factor	ACCF = 0	

No line search

TIMEINTEGRATION statement

Time integration	Backward	This set the time integration method for transient analysis
Number of time steps	Fixed time step = 50	The maximum number of discrete time integration steps to be calculated.
Starting time	0	The starting time is 0.
Time increment	0.001	The time increment is 0.001s.
Time stepping algorithm	Fixed	The time increment is fixed.

Convergence analysis

Because of the moving boundary, remeshing caused significant problems for every new mesh. Therefore, while we refined the mesh throughout the entire process we did no “final” mesh convergence check. After using many meshes (and seeing little difference between them and no strange effects in our final solution) we just stuck with the mesh we showed in this report.

Appendix D

[1] *What is Cancer?*. American Cancer Society, <http://www.cancer.org/docroot/home/index.asp>

[2][3] Reviewed 7/2/1999. *Cancer Facts* National cancer Institute, http://cis.nci.nih.gov/fact/7_8.htm

[4] *Laser Surgery*. Long Beach Animal hospital, <http://www.lbah.com/laser.htm>

Datta. A.K. 2003. *Computer-Aided Engineering: Applications to biomedical Processes*. Department of Biological and Environmental Engineering, Cornell University, Ithaca, New York.